European Review for Medical and Pharmacological Sciences 2015; 19: 1305-1314

The effect of Curcumin on NF-κB expression in rat with lumbar intervertebral disc degeneration

T. MA[1], C.-J. GUO[1], X. ZHAO[1], L. WU[1], S.-X. SUN[1], Q.-H. JIN[2]

[1]School of Clinical Medicine, Ningxia Medical University, Yinchuan, People's Republic of China
[2]Department of Orthopedics, General Hospital of Ningxia Medical University, Yinchuan, People's Republic of China

Abstract. – OBJECTIVE: To observe the effect of curcumin on the expression levels of nuclear factor κB-p65 (NF-κB-p65) and tumour necrosis factor α (TNF-α) in the nucleus pulposus in rats with lumbar intervertebral disc degeneration. And to investigate of the mechanism underlying the role of curcumin in decelerating the process of lumbar intervertebral disc degeneration.

MATERIALS AND METHODS: The model of lumbar intervertebral disc degeneration was established in Sprague-Dawley (SD) rats followed by a curcumin treatment. The ultra-microstructure histomorphological variations in the lumbar intervertebral disc of SD rats were evaluated. The protein and gene expression levels of NF-κB-p65 and TNF-α in the lumbar intervertebral disc were measured.

RESULTS: Magnetic resonance imaging (MRI) and histomorphology confirmed the establishment of a successful lumbar intervertebral disc degeneration model. The results from the MRI and the ultra-microstructures revealed a significant improvement in lumbar intervertebral disc degeneration in the curcumin-treated groups (low dose and high dose). No significant change was observed in the solvent control group treated with dimethyl sulfoxide (DMSO) alone. Based on the results of Western blot analysis and real-time PCR, the curcumin treatment (low dose and high dose) significantly reduced the expression levels of NF-κB-p65 and TNF-α in the lumbar intervertebral disc tissue compared with the groups without curcumin treatment and with the DMSO treatment alone. No significant difference, however, was observed between the low-dose and high-dose curcumin treatment groups.

CONCLUSIONS: Curcumin may inhibit the activation of NF-κB by inhibiting the translocation of NF-κB-p65 and reducing the release of inflammatory factors which, thereby, decelerates the process of lumbar intervertebral disc degeneration.

Key Words:
Curcumin, Degenerated lumbar intervertebral disc, NF-κB, TNF-α.

Introduction

Lumbar disc herniation and discogenic pain are common clinical diseases with a pathological basis of lumbar intervertebral disc degeneration. One characteristics of a degenerated lumbar intervertebral disc is the increased expression of typical NF-κB target genes, such as inflammatory factors, matrix metalloproteinase (MMP) and aggrecanases[1-4]. A previous study showed that a large amount of NF-κB accumulates in the degenerated lumbar intervertebral disc tissues, especially in the nucleus pulposus tissues, compared with normal lumbar intervertebral disc tissue[5]. NF-κB has been suggested to be a key transcription factor that can activate the IL-1β and TNF-α pathway to exert a key effect during lumbar intervertebral disc degeneration[6-8]. TNF-α has been suggested to play an important role in regulating cellular immunity and systemic inflammation[9]. A previous study confirmed that TNF-α was the major inflammatory factor in the mechanism responsible for the spinal nerve root pain caused by damaged nerve roots[10]. TNF-α has also been suggested to be an inducer of lumbar intervertebral disc degeneration[11]. The heterodimer p50-p65 has been suggested to be the most abundant form of NF-κB and was shown to control the expression of most of the genes[12]. Currently, no consensus treatment can decelerate the lumbar intervertebral disc degeneration process.

Curcumin is a natural polyphenol product extracted from *rhizoma curcumae longae* and is the major component of curry powder. It is orange in colour and has been used to treat various diseases, such as tumours and rheumatism[13]. Can curcumin treatment also decelerate the lumbar intervertebral disc degeneration process? In this study, an inhibition effect of curcumin on the NF-κB pathway was revealed in a rat lumbar in-

Corresponding Author: Qun-hua Jin, MD; e-mail: jinqunhua@sina.com

tervertebral disc degeneration model treated with curcumin. The molecular mechanism underlying the effect of curcumin to delay lumbar intervertebral disc degeneration is also preliminarily discussed.

Materials and Methods

Materials

The major reagents included the following: rabbit anti-rat NF-κB-p65 monoclonal antibody, rabbit anti-rat TNF-α monoclonal antibody, and alkaline phosphatase labelled goat anti-rabbit IgG (Beijing Biosynthesis Biotechnology Co., Ltd. China); reverse transcription kit and fluorescence quantitative mix (Beijing ZSGB-Bio Co., Ltd. China); curcumin (98% pure) solvated with a small amount of the assistant solvent DMSO (Xi'an Yuensun Biological Technology Co., Ltd. China).

Animals

Sixty male Sprague-Dawley (SD) rats (6-8 weeks old, weighing 190-220 g) were supplied by The Animal Experimental Centre of Ningxia Medical University. The animal experimental environment was of a clean grade. The rats were raised in temperature-controlled (22 ± 2°C) animal houses under 12:12 h light: dark cycles. The SD rats were randomly divided into the following 5 groups: normal control group (NC group, n=12), intervertebral disc degeneration group (IVD group, n=12), solvent control group (DMSO group, n=12), low-dose curcumin-treated group (LDCT group, n=12) and high-dose curcumin-treated group (HDCT group, n=12).

Establishment of the Lumbar Intervertebral Disc Degeneration Model

From each of the 5 groups, 2 SD rats were randomly selected, examined using MRI and properly labelled. The rats in all groups except the NC group underwent a surgical operation to establish the lumbar intervertebral disc degeneration model based on the method proposed by Chen et al[14]. Anaesthesia (3 ml/kg) was administered to the rats as an intraperitoneal injection of 10% chloral hydrate. Once the rats were anaesthetised, they were placed in a prone position with fixed limbs. A 4 cm × 8 cm area on the back skin was prepared using a depilatory. A sterilised cover sheet was then placed on the rats, and a midline incision was cut along the spinous processes of the back waist. After cutting the skin, a subperiosteal dissection was performed to sufficiently expose the L1-L6 spinous processes, the articular processes and the vertebral lamina. A rongeur was used to remove the spinous processes, the articular processes, the supraspinous ligaments and the interspinous ligaments. The bilateral erector spinae muscles were cut through. The subcutaneous fascia and skin were then stitched back together layer by layer. The NC group was excluded from special treatment. Once again, the rats were randomly divided into 4 groups after the surgery. After the surgery, the wound dressings were continuously changed on all of the rats for 3 days.

Drug administration methods: After the animal model was established, the LDCT and HDCT groups were given an intraperitoneal injection of 50 mg/kg and 100 mg/kg curcumin, respectively. The DMSO group was administered the same amount of DMSO by intraperitoneal injection. The NC group was excluded from any treatment. Six weeks later, an MRI examination was again performed on the labelled rats. All rats were then sacrificed. The lumbar intervertebral disc tissue was collected and divided into 5 groups with 3 fragments in each group. One fragment was immediately fixed in 2% glutaraldehyde, and the other 2 fragments were stored at –80°C.

Electron microscopy (EM) Examination

After the lumbar intervertebral disc tissue was fixed in 2% glutaraldehyde for 2 h and the protein tissues in the nucleus pulposus were completely denatured and solidified, the nucleus pulposus tissue was isolated (this approach may protect the nucleus pulposus tissue from damage and allow tissue fixation in a timely manner), washed with 0.1 mmol/L sodium phosphate buffer 3 times and fixed overnight. The samples were then fixed in 1% osmic acid, gradually dehydrated with ethanol and embedded in epoxy resin 618. Semi-thin sections of the embedded samples were collected and stained with toluidine blue. Under an optical microscope, the nucleus pulposus tissue was located; then, ultrathin sections were collected and double stained with uranyl acetate and lead citrate. The sections were observed and photographed under an electron microscope.

Western Blot Analysis

The nucleus pulposus tissue was collected from the lumbar intervertebral disc tissue stored at –80°C, weighed and ground. The protein con-

centration was determined using BCA methods following the instructions on the protein extraction kit and quantitative kit. The protein samples were mixed with 5 × SDS gel loading buffer, denatured at 100°C for 5 min, electrophoresed, transferred onto a PVDF membrane at 400 mA for 30 min and blocked in the TBS-T buffer with 5% fat free milk at room temperature for 1 h. The primary antibodies for NF-κB-p65 (1:500) and TNF-α (1:1000) were added, and the samples incubated at 4°C overnight. The membrane was washed with TDST before the secondary antibody (1:2000) was added, and the samples then incubated for 1 h at room temperature. The membrane was again washed with TDST. The PVDF membrane with ECL illuminant was then placed on a gel imaging analyser for exposure and imaging. The acquired images were processed with GraphPad Prism 5 software to obtain the grayscale value of each band from the samples. β-actin was used as an internal reference.

Real time Fluorescent Quantitative PCR (RT-PCR)

The nucleus pulposus tissue was collected from the lumbar intervertebral disc tissue stored at –80°C, weighed, ground, and the total RNA was extracted following the instructions from the fluorescent quantitative kit. The total RNA concentration and purity were determined using a spectrophotometer. The purity of the total RNA was verified based on an A260/A280 value between 1.8-2.0. Based on the instructions in the reverse transcription kit, the total RNA was then mixed into a 20 μL reaction system, reverse transcribed into cDNA, amplified and analysed. Glyceraldehyde 3-phosphate dehydrogenase (GAPDH) was used as internal reference. RNA primers for NF-κB-p65 and TNF-α were designed and synthesised by Shanghai Sangon Biotech, Co., Ltd., China. The forward primer for NF-κB-p65 was 5'-GCTATAATCCTGGACTTCTG-3'. The reverse primer for NF-κB-p65 was 5'-GAGGAAGGCTGTGAACATGA-3'. The forward primer for TNF-α was 5'-TGCTATCTCATACCAGGAGA-3'. The reverse primer for TNF-α was 5'-GACTCCGCAAAGTCTAAGTA-3'. The forward primer for GAPDH was 5'-TGGAGTCTACTGGCGTCTT-3'. The reverse primer for GAPDH was 5'-TGTCATATTTCTCGTGGTTCA-3'. Deionised water was used as a negative control. The reaction program was an initial denaturation at 95°C for 3 min, followed by 40 cycles of denaturation at 95°C for 30 s, annealing at 58°C for 30 s and extension at 75°C for 1 min and a final extension at 75°C for 5 min. The product was maintained at 4°C at the end of the program. The Ct values and the solvation curve that represented the specificity of gene products were automatically generated by a computer. The experimental results were expressed with a relative quantification method using $2^{-\Delta\Delta Ct}$.

Statistical Analysis

Statistical analyses were performed on the data acquired in this experiment using the SPSS 17.0 statistics software suite (SPSS Inc., Chicago, IL, USA). Measurement data were expressed as the mean ± standard deviation (±S). Measurement data for multiple groups were analysed and compared with squared deviations. When a comparison between groups revealed significant differences, the SNK method was used for pairwise comparisons. The significance level was set as $\alpha = 0.05$, and a $p < 0.05$ was considered statistically significant.

Results

Variations in the Lumbar Intervertebral Discs from Each Group Observed by MRI

Variations in the lumbar intervertebral discs from each group were seen in Figure 1.

Ultra-Microstructural Observation of Lumbar Intervertebral Disc Degeneration

Ultra-microstructural observations were shown in Figures 2, 3 and 4.

NC group: the histomorphology of the notochord cells mostly appeared as irregular shapes with round nuclei and uniform distribution of the nuclear chromatin. The cytoplasm contained a large amount of glycogen granules and various cellular structures, such as rough endoplasmic reticulum, mitochondria and the Golgi complex. Many villous pseudopod protrusions were stretched out around the extracellular surface (Figure 3, A2). A cartilage lacuna was observed around the chondrocyte-like cells. The nuclei of these cells were mostly spherical or oval in shape with a uniform distribution of the nuclear chromatin. The cytoplasm of the cells contained a sufficient rough endoplasmic reticulum. The mitochondria exhibited an oblong shape and visible ridge-like structures indicative of good activity. Glycogen granules and lipid droplets were scat-

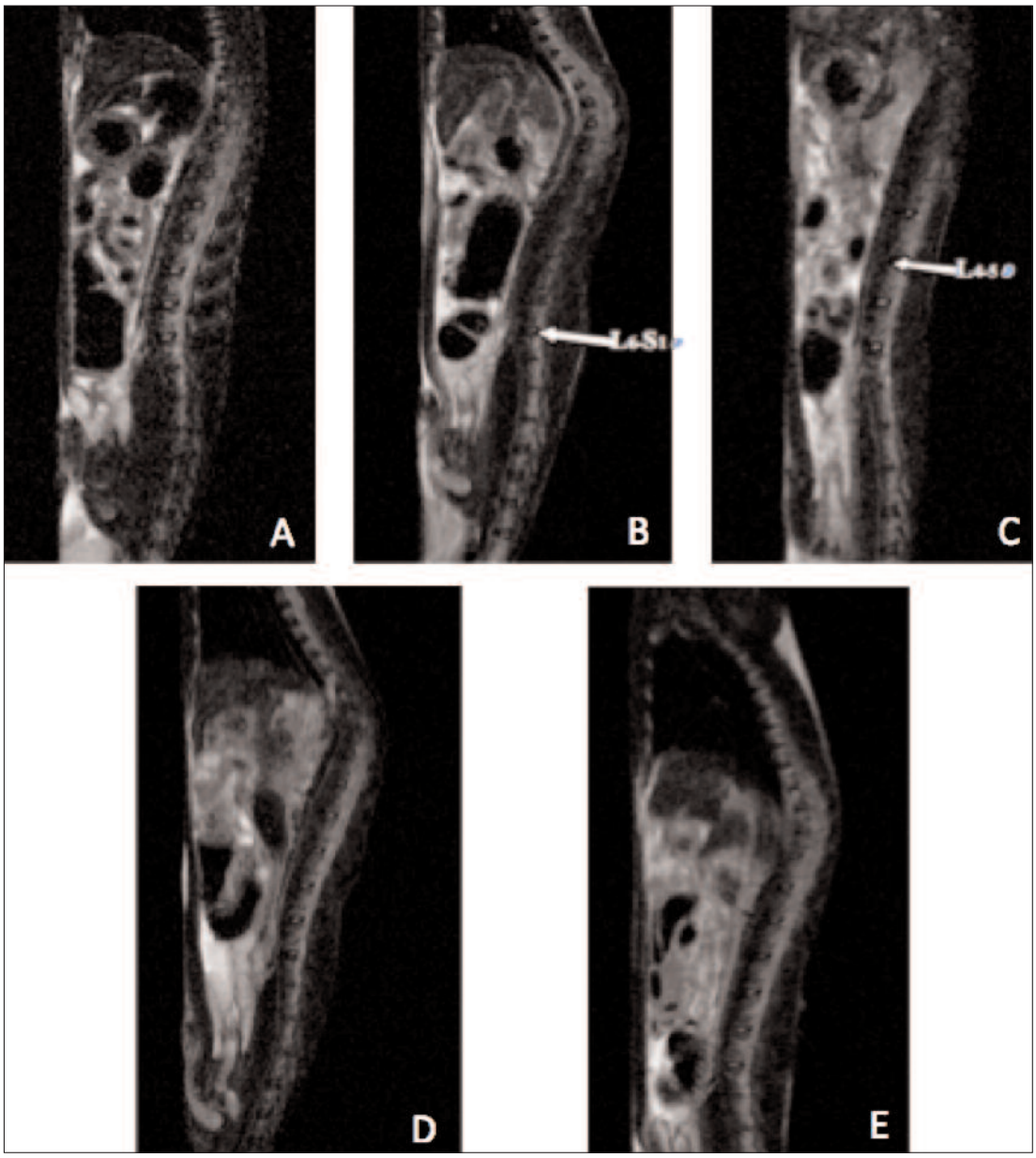

Figure 1. Rat lumbar MRI at T2W1, sagittal view. ***A,*** NC group before surgery, high signals were observed at the normal lumbar intervertebral disc. ***B,*** Postsurgical IVD group, significantly low signals were observed at the lumbar intervertebral disc (L1-6). ***C,*** Postsurgical DMSO group, significantly lower signals were observed at the lumbar intervertebral disc (L1-5) compared with the NC group. ***D,*** Postsurgical LDCT group, signals at the lumbar intervertebral disc (L1-6) were slightly lower than those in the NC group but were significantly higher than those in the IVD group. ***E,*** Postsurgical HDCT group, signals at the lumbar intervertebral disc (L1-6) were slightly lower than those in the normal group but were significantly higher than those in the IVD group. No significant difference was observed between the HDCT and LDCT groups.

tered in the cytoplasm (Figure 4, A3). The collagen fibres around the notochord cells appeared to be neat and orderly. Stripes between collagen fibres were clearly visible (Figure 2, A1).

IVD group: Notochord cells were rarely observed and their nuclei demonstrated different degrees of shrinkage with invaginated nuclear membrane. The intranuclear heterochromatin was aggregated. The amount of intracellular glycogen granules was significantly greater. The cytoplasm of the cells was filled with a large number of vacuoles (Figure 3. B2). The heterochromatin in the nuclei of the chondrocyte-like cells was decreased. The cells exhibited dilation

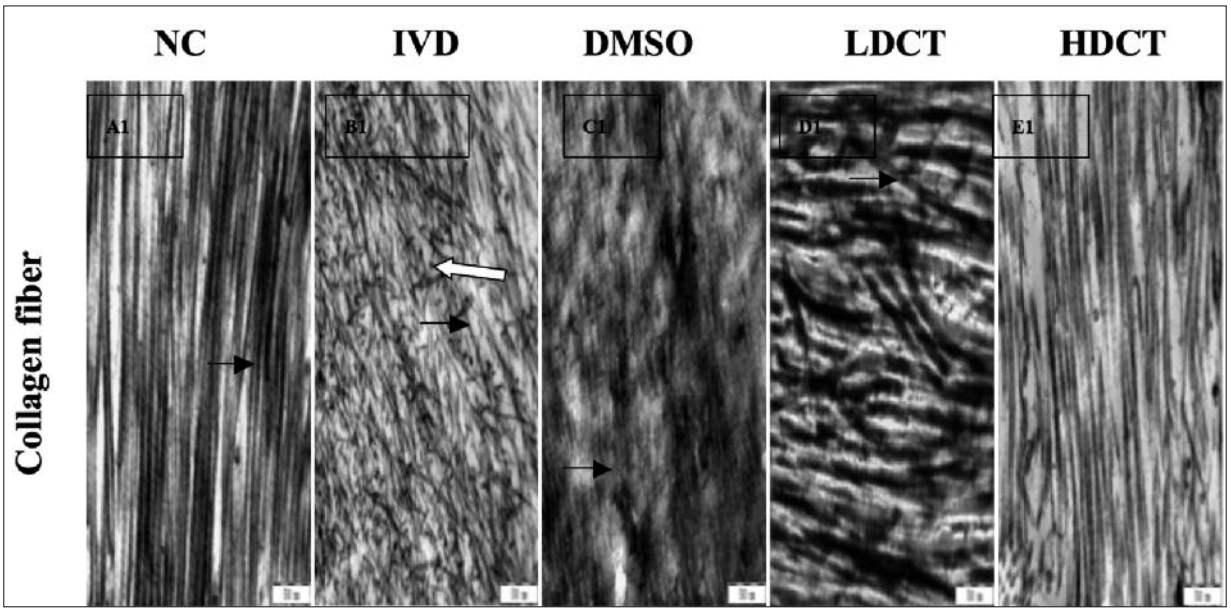

Figure 2. Ultra-microstructures of the collagen fibres in the five groups. ***A1,*** The black arrow in the NC group indicates the normal collagen fibres. ***B1,*** The black arrow in the IVD group indicates the degenerated collagen fibres that appear to be thin and long; the white arrow indicates the short, small aggregated collagen fibres. ***C1,*** The black arrow in the DMSO group indicates the collagen fibres with morphological change due to calcification, exhibiting no fibril gaps, ***D1,*** The black arrow in the LDCT group indicates structures for comparison with the normal collagen fibres. ***E1,*** The collagen fibres in the HDCT group were worse than those in the NC group but showed significant improvement compared with those in the IVD, DMSO and LDCT groups. (8000×).

of the rough endoplasmic reticulum, an increase in the number of lysosomes and a decrease in the number of mitochondria and glycogen granules. The size of the chondrocyte-like cells was reduced, and the cells exhibited necrotic changes with many vacuoles. The cells appeared to be arranged in "nest-like" thickened multiple layers. The fibre tissues in this group were thinner and

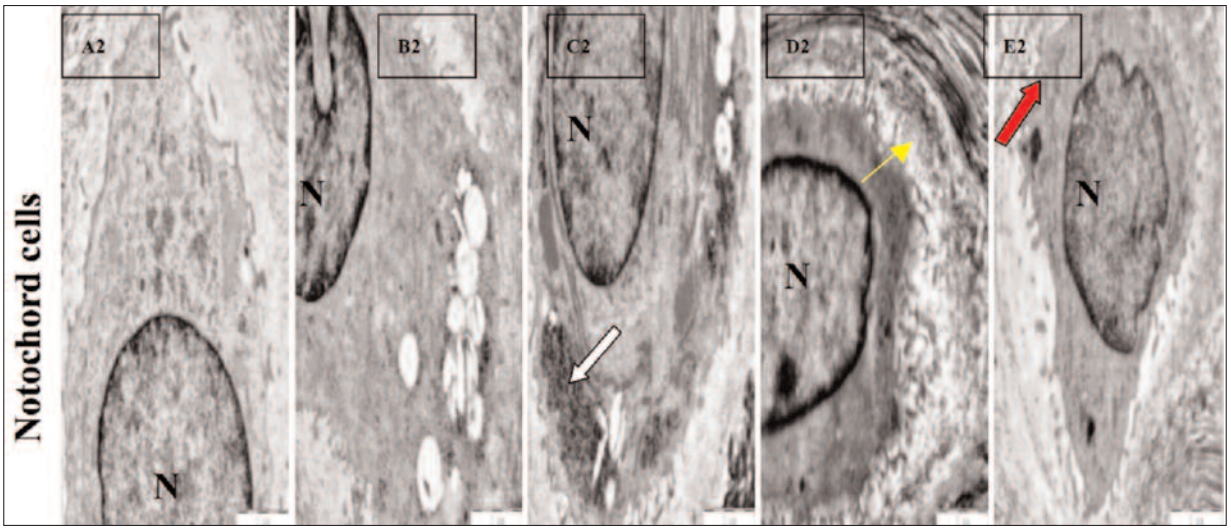

Figure 3. N indicates the nucleus; the black arrow in ***B2*** indicates vacuoles; the white arrow in ***C2*** indicates the significant decrease in glycogen; the yellow arrow in ***D2*** indicates the "nest-like" thickening around the nucleus; the red arrow in ***E2*** indicates the rough endoplasmic reticulum. (2500×).

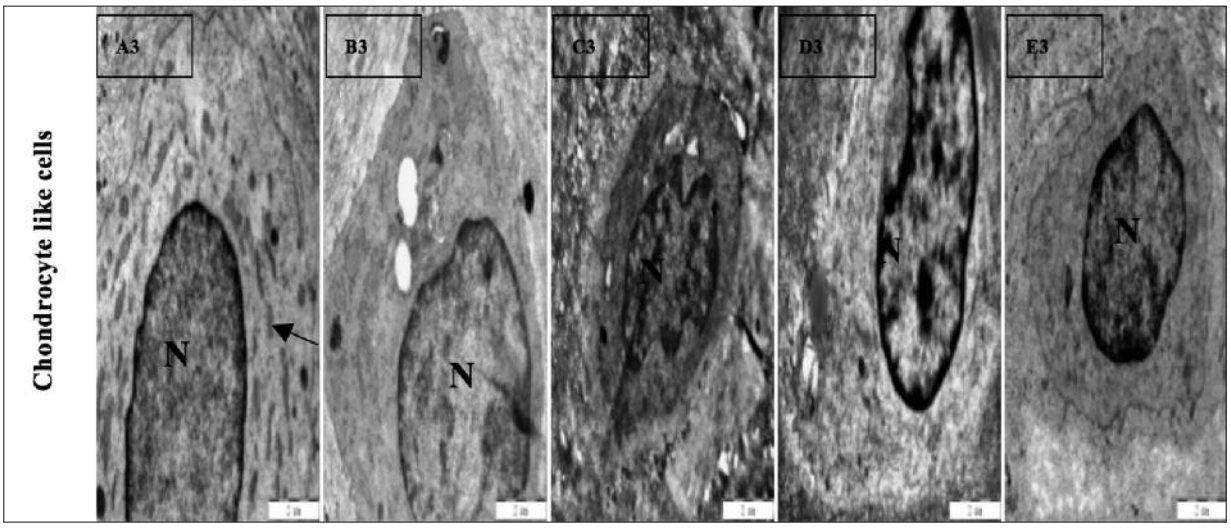

Figure 4. The black arrow in A3 indicates the rough endoplasmic reticulum in the normal cell structure, N indicates the nucleus. (2500×).

shorter compared with the collagen fibres in normal tissue. The fibres were branched, scattered, and disorderly arranged (Figure 2, B1).

LDCT and HDCT groups: The nuclei of the notochord cells exhibited deformities with shrinkage and intranuclear heterochromatin aggregation. The amount of rough endoplasmic reticulum in the cells was reduced, and the number of mitochondria and the amount of glycogen were also decreased. A small number of vacuoles were observed in the cytoplasm (Figure 3). These conditions, however, were significantly better than those in the IVD group. The chondrocyte-like cells were small, their nuclei were shrunken and the intranuclear heterochromatin was aggregated. No significant dilation of the rough endoplasmic reticulum was observed in these cells. The glycogen level was reduced. The collagen fibres were slightly thicker than those in the NC group but were significantly better than those in the IVD group. No significant difference was observed between the HDCT group and the LDCT group. The collagen fibres observed in these two groups were worse than those the NC group with many filament fibres that were orderly arranged. Stripes between collagen fibres were also clearly visible, which was a significant improved compared with those in the IVD group and DMSO group. The results observed in the HDCT group were slightly better than those observed in the LDCT group.

DMSO group No significant difference was observed in the notochord cells or chondrocyte-like cells in the DMSO group compared with those in the IVD group. The degree of degeneration in this group was worse than that observed in the HDCT, LDCT and NC groups. The collagen fibres exhibited significant calcification changes and were in a compact arrangement.

Results of the Real Time Fluorescent Quantitative PCR

The mRNA expression levels of NF-κB-p65 and TNF-α were determined using fluorescent quantitative RT-PCR. Upon comparing the 5 groups, the groups treated with curcumin had significantly lower mRNA expression levels than the other groups ($p < 0.05$), as shown in Figure 5.

Western Blot Analysis Results

NF-κB-p65 and TNF-a were only weakly expressed in the NC group, and their expression levels were significantly higher in the IVD group compared with the other groups. The expression levels of NF-κB-p65 and TNF-α were significantly lower in the LDCT and HDCT groups compared with the IVD group, and this difference was statistically significant ($p < 0.05$) (Figure 6). No significant difference was observed between the LDCT and HDCT groups.

Discussion

NF-κB has been shown to initiate the transcription processes of many genes related to the immune response, the expression of inflammatory molecules and the proliferation and anti-apop-

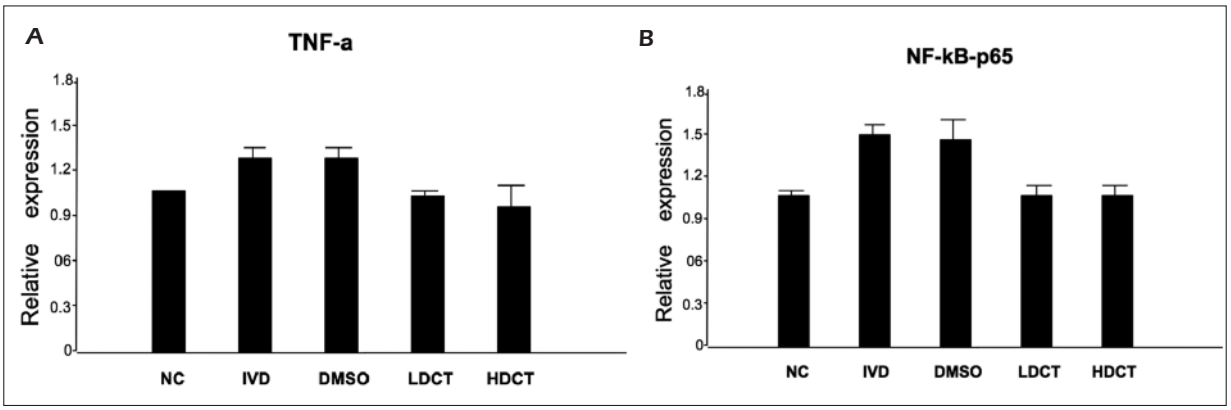

Figure 5. ***A, B,*** The mRNA expression levels of NF-κB-p65 and TNF-α in each group detected by qRT-PCR.

tosis of cells[15]. When cells experience stimuli such as oxidation, pressure, genetic toxins, and mechanical and chemical stresses, IκB is released from the trimer. The translocation signal on the p50 subunit and the DNA binding pocket on the p65 subunit are thereby exposed. Through this mechanism, the remaining heterodimer demonstrates NF-κB activity and begins to translocate from the cytoplasm to the nucleus to bind to κB sequences and exert its transcription regulatory effect[16]. In an animal study, Nasto et al[17] showed that the NF-κB signal pathway was very important in age-related lumbar intervertebral disc degeneration. In an equivalent gene knock-out mouse model of accelerated lumbar intervertebral disc degeneration, the application of the NF-κB-p65 inhibitor Nemo Binding Domain (NBD) significantly decelerated the lumbar intervertebral disc degeneration process. Therefore, we suggest that NF-κB-p65 and TNF-a play important roles during the entire pathological process of lumbar intervertebral disc degeneration. To further confirm the different expression levels of NF-κB-p65 and TNF-α between the degenerated lumbar intervertebral disc and the normal lumbar intervertebral disc, we performed a Western blot analysis and RT-PCR experiments to compare the protein and mRNA expression levels of NF-κB-p65 and TNF-α. The results revealed that the expression levels of NF-κB-p65 and TNF-α in the IVD and DMSO groups were significantly higher than those in the normal groups and were significantly different from those in the HDCT group and LDCT group.

Singh et al[18] first reported that curcumin could down-regulate the TNF-α induced activities of NF-κB and AP-1. Another previous study showed that the application of curcumin in endothelial cells to inhibit the TNF-α-induced NF-κB activity could effectively reduce the expression of NF-κB[19]. In a previous rat study on liver and kidney dysfunction caused by cecal perforation-induced sepsis, Savcun et al[20] administered curcumin by intraperitoneal injection and observed significant decreases in TNF-α IL-1β expression in the liver. After the curcumin treatment in this study, the expression levels of NF-κB-p65 and TNF-α in the nucleus pulposus of

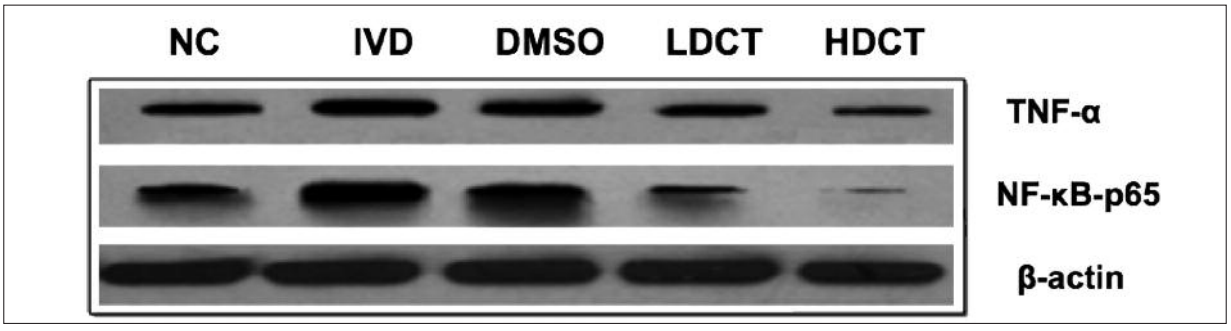

Figure 6. The protein expression of NF-κB-p65 and TNF-α was detected by Western blot and their relative expression was normalized.

Table I. RT-PCR relative quantification results ($\bar{x} \pm s$).

Group	N	TNF-α gene	NF-κB-p65 gene
NC	12	1.113 ± 0.106	1.058 ± 0.111
DMSO	12	2.748 ± 0.043*	2.851 ± 0.199*
IVD	12	2.888 ± 0.044*,▲	2.842 ± 0.228*
LDCT	12	1.437 ± 0.020*,▲,☆	1.422 ± 0.116*,▲,☆
HDCT	12	1.269 ± 0.028*,▲,☆,Δ	1.269 ± 0.113*,▲,☆,Δ
F value		2698.312	361.758
p value		0.000	0.000

Note: A pairwise comparison was performed using the SNK method; *Indicates a significant difference compared with the NC group; ▲Indicates a significant difference compared with the DMSO group; ☆Indicates a significant difference compared with the IVD group; ΔIndicates a significant difference compared with the LDCT group.

the degenerated lumbar intervertebral disc were significantly lower than the levels in the IVD group and DMSO group. These differences were statistically significant. Additionally, the lumbar MRI on the rats 6 weeks before and after surgery confirmed that the curcumin treatment significantly improved lumbar intervertebral disc degeneration.

The rough endoplasmic reticulum is known to participate in protein synthesis and matrix construction and repair. The mitochondria are known to participate in supplying the energy necessary for life activities. The dilation of and decrease in the rough endoplasmic reticulum and the increases in the numbers of lysosomes and intranuclear vacuoles reflect a direct change in the cellular organelles after lumbar intervertebral disc degeneration[21]. In this study, the ultra-microstructure of early lumbar intervertebral disc degeneration revealed a large increase in the amount of mucopolysaccharide in the notochord cells, which is consistent with a previous study by Allon et al[22] that discovered an increase in the amount of mucopolysaccharide in degenerated lumbar intervertebral discs. After the curcumin treatment, a reduced number of lysosomes and vacuoles and a reduction in the dilation of rough endoplasmic reticulum were observed through the ultra-microstructure analysis of notochord cells. Meanwhile, no increase in the amount of mucopolysaccharide was observed in the degenerated notochord cells in the curcumin-treated groups compared with the typical mucopolysaccharide increase observed in lumbar intervertebral disc degeneration.

This study had a few limitations. First, the surgical approach used to generate the lumbar intervertebral disc degeneration model lacked a further verification of the type of lumbar intervertebral disc degeneration and the categorisation of such degeneration in the MRI. Additionally, no statistical analysis was performed on the differences between each lumbar intervertebral disc studied in the MRI experiment. The variations in the ultra-microstructures of the different types of lumbar intervertebral discs also required further statistical analysis to verify the differences. Despite these limitations, the results from this ex-

Table II. Western Blot quantification results for each group ($\bar{x} \pm s$).

Group	N	TNF-α gene	NF-κB-p65 gene
NC	12	1.039 ± 0.026	1.150 ± 0.016
DMSO	12	1.228 ± 0.036*	1.470 ± 0.013*
IVD	12	1.191 ± 0.014*,▲	1.485 ± 0.021*
LDCT	12	0.969 ± 0.014*,▲,☆	1.013 ± 0.051*,▲,☆
HDCT	12	0.951 ± 0.011*,▲,☆	0.990 ± 0.075*,▲,☆
F value		394.037	386.622
p value		0.000	0.000

Note: A pairwise comparison was performed using the SNK method; *Indicates a significant difference compared with the NC group; ▲Indicates a significant difference compared with the DMSO group; ☆Indicates a significant difference compared with the IVD group; ΔIndicates a significant difference compared with the LDCT group.

periment clearly demonstrate degeneration in L1-L6 in the surgical model groups compared with the NC group. Degeneration in T12-L1, L1-2, and L3-4 was also observed in the DMSO group compared with the NC group. After the surgery, all of the lumbar intervertebral discs in the IVD and DMSO groups exhibited degeneration and noticeable collapses were observed in the thoracic vertebrae from the MRI. Correlations between the LDCT and HLCT groups may exist, but a further study optimising the curcumin dosage is necessary. Finally, this study did not extensively investigate the drug administration routes or monitor the events at the key time points after drug injection.

Conclusions

Based on the Western blot analysis, ultra-microstructure EM and real time-PCR results, this animal study shows that curcumin can decelerate the degeneration process in lumbar intervertebral discs by inhibiting the NF-κB-p65 activity and reducing inflammatory factors. This study provides new evidence for the prevention and treatment of lumbar intervertebral disc degeneration.

Conflict of Interest

The Authors declare that there are no conflicts of interest.

References

1) Burke JG, Watson RW, McCormack D, Dowling FE, Walsh MG, Fitzpatrick JM. Intervertebral discs which cause low back pain secrete high levels of proinflammatory mediators. J Bone Joint Surg Br 2002; 84: 196-201.
2) Hoyland JA, Le Maitre C, Freemont AJ. Investigation of the role of IL-1 and TNF in matrix degradation in the intervertebral disc. Rheumatology 2008; 47: 809-814.
3) Zhao CQ, Zhang YH, Jiang SD, Li H, Jiang LS, Dai LY. ADAMTS-5 and intervertebral disc degeneration: the results of tissue immunohistochemistry and *in vitro* cell culture. J Orthop Res 2011; 29: 718-725.
4) Yurube T, Takada T, Suzuki T, Kakutani K, Maeno K, Doita M, Kurosaka M, Nishida K. Rat tail static compression model mimics extracellular matrix metabolic imbalances of matrix metalloproteinases, aggrecanases, and tissue inhibitors of metalloproteinases in intervertebral disc degeneration. Arthritis Res Ther 2012; 14: R 51.
5) Nerlich AG, Bachmeier BE, Schleicher E, Rohrbach H, Paesold G, Boos N. Immunomorphological analysis of RAGE receptor expression and NF-kappa B activation in tissue samples from normal and degenerated intervertebral discs of various ages. Ann N Y Acad Sci 2007; 1096: 239-248.
6) Hoyland JA, Le Maitre C, Freemont AJ. Investigation of the role of IL-1 and TNF in matrix degradation in the intervertebral disc. Rheumatology 2008; 47: 809-814.
7) Le Maitre CL, Freemont AJ, Hoyland JA. The role of interleukin-1 in the pathogenesis of human intervertebral disc degeneration. Arthritis Res Ther 2005; 7: R732-R745.
8) Le Maitre CL, Hoyland JA, Freemont AJ. Catabolic cytokine expression in degenerate and herniated human intervertebral discs: IL-1beta and TNFalpha expression profile. Arthritis Res Ther 2007; 9: R77.
9) Locksley RM, Killeen N, Lenardo MJ. The TNF and TNF receptor superfamilies: integrating mammalian biology. Cell 2001; 104: 487-501.
10) Igarashi T, Kikuchi S, Shubayev V, Myers RR. Exogenous tumor necrosis factor-alpha mimics nucleus pulposus-induced neuropathology molecular, histologic, and behavioral comparisons in rats. Spine 2000; 25: 2975-2980.
11) Hayashi S, Taira A, Inoue G, Koshi T, Ito T, Yamashita M, Yamauchi K, Suzuki M, Takahashi K, Ohtori S. TNF-alpha in nucleus pulposus induces sensory nerve growth: a study of the mechanism of discogenic low back pain using tnf-alpha–deficient mice. Spine 2008; 33: 1542-1546.
12) Baeuerle PA, Henkel T. Function and activation of NF-kappa B in the immune system. Annu Rev Immunol 1994; 12: 141-179.
13) Zhou H, Beevers CS, Huang S. The targets of curcumin. Curr Drug Targets 2011; 12: 332-347.
14) Chen DS, Jin QH, Zhang Y. Observation of ultrapathology in the rat mode l study of experimental lumbar intervertebral disc degeneration. Chinese J Exp Surg 2006; 23: 625-626.
15) Hayden MS, Ghosh S. Shared principles in NF-kappaB signaling. Cell 2008; 132: 344-362.
16) Hayashi S, Taira A, Inoue G, Koshi T, Ito T, Yamashita M, Yamauchi K, Suzuki M, Takahashi K, Ohtori S. TNF-alpha in nucleus pulposus induces sensory nerve growth: a study of the mechanism of discogenic low back pain using TNF-alpha-deficient mice. Spine 2008; 33: 1542-1546.
17) Nasto LA, Seo HY, Robinson AR, Tilstra JS, Clauson CL, Sowa GA, Ngo K, Dong Q, Pola E, Lee JY, Niedernhofer LJ, Kang JD, Robbins PD, Vo NV. ISSLS prize winner: inhibition of NF-κB activity ameliorates age-associated disc degeneration in a mouse model of accelerated aging. Spine 2012; 37: 1819-1825.
18. Singh S, Aggarwal BB. Activation of transcription factor NF-kappa B is suppressed by curcumin (diferuloylmethane). Biol Chem 1995; 270: 24995-25000.

19) Kumar A, Dhawan S, Hardegen NJ, Aggarwal BB. Curcumin (Diferuloylmethane) inhibition of tumor necrosis factor (TNF)-mediated adhesion of monocytes to endothelial cells by suppression of cell surface expression of adhesion molecules and of nuclear factor-kappaB activation. Biochem Pharmacol 1998; 55: 775-783.

20) Yilmaz Savcun G, Ozkan E, Dulundu E, Topalo lu U, Sehirli AO, Tok OE, Ercan F, Sener G. Antioxidant and anti-inflammatory effects of curcumin against hepatorenal oxidative injury in an experimental sepsis model in rats. Ulus Travma Acil Cerrahi Derg 2013; 19: 507-515.

21) Gruber HE, Hanley EN Jr. Observations on morphologic changes in the aging and degenerating human disc: secondary collagen alterations. BMC Musculoskelet Disord 2002; 3: 9.

22) Allon AA, Butcher K, Schneider RA, Lotz JC. Structured bilaminar coculture outperforms stem cells and disc cells in a simulated degenerate disc environment. Spine 2012; 37: 813-818.